Rescue of *Aspergillus nidulans* severely debilitating null mutations in ESCRT-0, I, II and III genes by inactivation of a salt-tolerance pathway allows examination of ESCRT gene roles in pH signalling

Ana M. Calcagno-Pizarelli[1], América Hervás-Aguilar[2,*], Antonio Galindo[2], Juan F. Abenza[2], Miguel A. Peñalva[2,‡] and Herbert N. Arst, Jr[1,‡]

[1]Section of Microbiology, Imperial College London, Flowers Building, Armstrong Road, London SW7 2AZ, UK
[2]Department of Molecular Medicine, Centro de Investigaciones Biológicas CSIC, Ramiro de Maeztu 9, Madrid, 28040, Spain
*Present address: Department of Molecular Biosciences, University of Kansas, Lawrence, KS 66045, USA
‡Authors for correspondence (penalva@cib.csic.es; h.arst@imperial.ac.uk)

Accepted 22 June 2011
Journal of Cell Science 124, 4064–4076
© 2011. Published by The Company of Biologists Ltd
doi: 10.1242/jcs.088344

Abstract

The *Aspergillus pal* pathway hijacks ESCRT proteins into ambient pH signalling complexes. We show that components of ESCRT-0, ESCRT-I, ESCRT-II and ESCRT-III are nearly essential for growth, precluding assessment of null mutants for pH signalling or trafficking. This severely debilitating effect is rescued by loss-of-function mutations in two cation tolerance genes, one of which, *sltA*, encodes a transcription factor whose inactivation promotes hypervacuolation. Exploiting a conditional expression *sltA* allele, we demonstrate that deletion of *vps27* (ESCRT-0), *vps23* (ESCRT-I), *vps36* (ESCRT-II), or *vps20* or *vps32* (both ESCRT-III) leads to numerous small vacuoles, a phenotype also suppressed by SltA downregulation. This situation contrasts with normal vacuoles and vacuole-associated class E compartments seen in *Saccharomyces cerevisiae* ESCRT null mutants. Exploiting the suppressor phenotype of *sltA*$^{-}$ mutations, we establish that Vps23, Vps36, Vps20 and Vps32 are essential for pH signalling. Phosphatidylinositol 3-phosphate-recognising protein Vps27 (ESCRT-0) is not, consistent with normal pH signalling in *rabB* null mutants unable to recruit Vps34 kinase to early endosomes. In contrast to the lack of pH signalling in the absence of Vps20 or Vps32, detectable signalling occurs in the absence of ESCRT-III subunit Vps24. Our data support a model in which certain ESCRT proteins are recruited to the plasma membrane to mediate pH signalling.

Key words: PacC processing, Multivesicular body pathway, Endosomes, Arrestin

Introduction

Endosomal sorting complexes required for transport (ESCRTs) play central roles in the biology of eukaryotic cells (Hurley and Emr, 2006; McDonald and Martin-Serrano, 2009; Rusten and Stenmark, 2009), of which possibly the most studied are the biogenesis of multivesicular endosomes and sorting of endosomal cargo destined for degradation in the lumen of the vacuole or lysosome (Hurley and Hanson, 2010; Katzmann et al., 2002).

One poorly understood role is that played by ESCRTs in fungal ambient pH signalling (denoted the *pal/RIM* pathway), which allows fungi to tailor gene expression to environmental pH (Peñalva et al., 2008; Peñalva and Arst, 2004). Activation of this pathway by alkaline pH ultimately results in the proteolytic processing activation of the transcription factor Rim101p in *Saccharomyces cerevisiae* (Li and Mitchell, 1997; Xu and Mitchell, 2001) and PacC in *Aspergillus nidulans* (Díez et al., 2002; Hervás-Aguilar et al., 2007; Orejas et al., 1995; Peñas et al., 2007). In *A. nidulans*, where ambient pH signalling has been thoroughly studied, the *pal* pathway involves six dedicated components. Of these, three constitute a 'sensor' plasma membrane complex, including the seven-transmembrane receptor (7-TMDR) PalH, a 'helper' 3-TMD protein PalI and the positive-acting arrestin PalF (Calcagno-Pizarelli et al., 2007; Herranz et al., 2005). The remaining three Pal proteins are interactors of ESCRT-III components. Thus, Bro1 domain-containing and YPXL/I motif-recognising protein PalA binds Vps32 (Vincent et al., 2003; Xu and Mitchell, 2001), as does Bro1-like protein PalC (Galindo et al., 2007), whereas calpain-like and almost certain signalling protease PalB binds Vps24 (Rodríguez-Galán et al., 2009). Pal–ESCRT-III interactions are required for efficient PacC proteolytic activation (Rodríguez-Galán et al., 2009), but the key role that ESCRT complexes are anticipated to play in pH signalling remains unanalysed because null ESCRT mutations, which were instrumental in establishing involvement in *S. cerevisiae* and *Candida albicans* Rim101 activation (Cornet et al., 2005; Hayashi et al., 2005; Kullas et al., 2004; Rothfels et al., 2005; Xu et al., 2004), are severely debilitating in *Aspergillus* (Rodríguez-Galán et al., 2009).

The nearly exclusive plasma membrane localisation of PalH in the presence of stoichiometric amounts of PalI (Calcagno-Pizarelli

This is an Open Access article distributed under the terms of the Creative Commons Attribution Non-Commercial Share Alike License (http://creativecommons.org/licenses/by-nc-sa/3.0), which permits unrestricted non-commercial use, distribution and reproduction in any medium provided that the original work is properly cited and all further distributions of the work or adaptation are subject to the same Creative Commons License terms.

Journal of Cell Science

Journal of Cell Science

et al., 2007), the PalH- and alkaline pH-dependent ubiquitylation of the PalF arrestin (Herranz et al., 2005), and the involvement of ESCRTs shown in yeasts has led to models in which attachment of ubiquitin (a well-established endocytic sorting signal) to PalF (Rim8 in yeasts) drives internalisation of the PalH–PalF complex, leading to organisation of an ESCRT-associated endosomal complex promoting proteolytic processing activation of PacC/Rim101 (Mitchell, 2008; Peñalva et al., 2008). Newer evidence strongly indicates that the pH signalling role of ESCRTs takes place at the plasma membrane. First, the Vps32 interactor PalC localises to cortical punctate structures at the plasma membrane (rather than to endosomes) in an ambient pH- and PalH-dependent manner (Galindo et al., 2007) and thus ESCRT recruitment to plasma membrane pH signalling sites would explain this conundrum. Second, PalF promotes the localisation of PalH to the plasma membrane, rather than to endosomes (Hervás-Aguilar et al., 2010a). Third, Rim8p (yeast PalF) binds Vps23p, Rim8p ubiquitylation contributes to this binding, and overexpressed Rim8p and Vps23p colocalise at cortical sites (Herrador et al., 2009). Fourth, attachment of an ubiquitin molecule to PalF leads to constitutive activation of the pathway, which correlates with recruitment of PalC to cortical sites (Hervás-Aguilar et al., 2010a).

Thus, the attractive possibility that ESCRTs play a role at the plasma membrane without promoting membrane budding (as during HIV-1 release) requires further investigation. The more robust physiological pH responses and the much larger size of the hyphal tip cells of *A. nidulans* compared to yeast cells make it ideal for these studies, thus far precluded by the fact that, as we demonstrated here for key components of ESCRT-0, ESCRT-I, ESCRT-II and ESCRT-III, *A. nidulans* null ESCRT mutations are severely debilitating. However, we show that second-site mutations in genes involved in a filamentous fungal-specific salt-tolerance pathway rescue this debilitation, enabling us to examine involvement of key components of the ESCRT pathway in proteolytic processing activation of PacC.

Results

Lack of a key component of any of the four ESCRT complexes is severely debilitating in *Aspergillus nidulans*

We replaced the coding regions of the *A. nidulans vps27* (ESCRT-0), *vps23* (ESCRT-I), *vps36* (ESCRT-II) and *vps20* and *vps32* (both ESCRT-III) genes by *Aspergillus fumigatus pyrG*, selecting for pyrimidine prototrophy. Vps27 initiates the multivesicular body (MVB) pathway. Vps23 plays a central role in the MVB pathway by binding Vps27, ubiquitylated cargo and the other components of ESCRT-I but, importantly, Vps23 appears to be involved in recognising the ubiquitylated forms of Rim8/PalF arrestins (Herrador et al., 2009; Hervás-Aguilar et al., 2010a), thus triggering the ambient pH signalling pathway at the plasma membrane. Vps36 contains a split PH domain that cooperates to recruit ESCRTs to phosphatidylinositol 3-phosphate [PtdIns(3)*P*]-containing endosomal membranes. Vps32 is the major structural component of the ESCRT-III polymeric lattice, whereas Vps20 is thought to initiate Vps32 polymerisation, coupling it to ESCRT-II (Teis et al., 2008). In all cases we obtained two types of primary transformants. One type grew very slowly and failed to conidiate. The other type had a typically heterokaryotic morphology. Plating conidiospores (individual nuclei of the coenocytic vegetative mycelium segregate into uninucleate conidiospores) of this second type on pyrimidine-free medium yielded the type 1 slow-growing aconidial colonies seen on the transformation plates (supplementary material Fig. S1 shows data for *vps32Δ*), strongly indicating that slow-growers carry the deletion in homokaryosis and thus that any of the five tested gene deletions is severely debilitating.

Growth and conidiation of *vpsΔ* strains can be greatly improved by extragenic suppressor mutations

Upon prolonged incubation, the growth and conidiation of many of the poorly growing, aconidial *vpsΔ* transformants improved markedly, suggesting that suppressor mutations might be arising spontaneously (supplementary material Fig. S1, *vps32Δ*). Southern and PCR analyses confirmed deletion of the target *vps* gene in each case (supplementary material Fig. S1 and data not shown). In every case except for *vps32Δ* (it appears that unsuppressed *vps32Δ* is lethal in ascospores), outcrossing to a wild-type strain yielded four classes of progeny: wild type; suppressed *vpsΔ* strains resembling the parent; slow-growing, aconidial *vpsΔ* strains; and *vps*$^{+}$ strains carrying the suppressor mutation. For example, for *vps36Δ sltA52* we scored, among $n=40$ progeny of a cross with a wild-type strain, ten *vps36Δ*, nine *vps*$^{+}$ *sltA*$^{+}$, ten *sltA52* and 11 *vps36Δ sltA52* colonies. These data strongly indicate that suppression resulted from mutations in one or more genes recombining freely with the corresponding *vps* locus.

The sensitivity to high concentrations of Na^{+}, K^{+} and L-arginine that suppressor mutations were found to confer provided a valuable indicator for their identification because these phenotypic features characteristically result from mutations in the *sltA* gene encoding a zinc-finger transcription factor involved in cation homeostasis (Findon et al., 2010; O'Neil et al., 2002; Spathas, 1978; Spielvogel et al., 2008). Sequence analysis of *sltA* in suppressor strains confirmed that a majority of the suppressors result from loss-of-function mutations in *sltA* (Fig. 1B). Fig. 1A shows the sensitivity of these single *sltA*$^{-}$ mutant strains to 1 M NaH_2PO_4 (this sensitivity is one diagnostic test for *sltA* function), compared with that shown by a null *sltAΔ* strain. *sltA51* and *sltA58* largely resemble the null strain in their inability to grow under these conditions (Fig. 1A), in agreement with the fact that they lead to early SltA truncation, which removes the complete DNA binding domain (Fig. 1B). *sltA52* and *sltA59*, neither of which remove the zinc-finger region, show a weaker phenotype (Fig. 1A). *sltA52* leads to a single residue substitution involving a residue in the reading α-helix of zinc-finger 3 whereas *sltA59* removes the ~90 C-terminal residues (Fig. 1B). *sltA54*, which removes only the 64 C-terminal residues, showed the weakest phenotype (Figs 1, 2). These and data below unambiguously established that strong *vpsΔ* suppression does not require the complete loss of *sltA* function.

All of the remaining suppressor mutations occur in a gene that we denoted *sltB* (e.g. *sltB53* was isolated as suppressor of *vps20Δ*). *sltA* and *sltB* null mutations are phenotypically indistinguishable and they are not additive in double mutants, indicating that *sltA* and *sltB* act in the same pathway (data not shown). Of note, like *sltA*$^{-}$ mutations (Findon et al., 2010), *sltB*$^{-}$ mutations result in a marked increase in the volume of the vacuolar system (A.M.C.-P., H.N.A. and M.A.P., unpublished results, and see below). In this paper, we focus on ESCRT function. A detailed characterisation of *sltB* and the *sltA–sltB* pathway will be reported elsewhere.

Journal of Cell Science

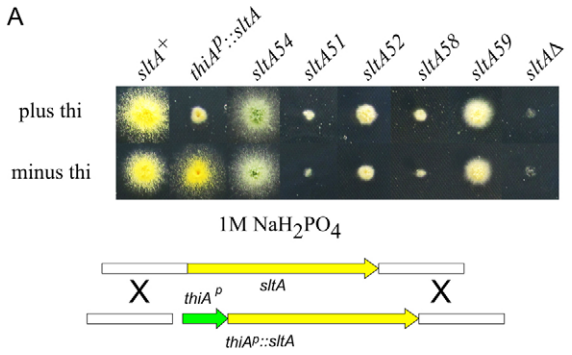

B

Truncating mutations			Missense mutations	
Allele	DNA change	Protein	DNA change	Substitution
sltA50	C54*ins*ACCCGAGGCGCCC	P19fs		
sltA51	Δ(C501 -T502)	S165fs		
sltA52			C1585G	Q494E
sltA54	G3359*ins*G	D634fs		
sltA55			T1609C	W502R
sltA58	ΔA829	T260fs		
sltA59	G1927T	Q607*		
sltA60	G1927T	Q607*		

New mutations characterised in *sltA*

Fig. 1. Na^+ tolerance phenotypes of *sltA* alleles. (**A**) Strains were cultured at 37℃ on synthetic complete medium containing 1 M NaH_2PO_4 with or without 100 μM thiamine (thi), i.e. under repressing and non-repressing conditions for *thiA^p::sltA*. The gene replacement procedure used to place *sltA* under the control of *thiA^p* (green) is shown schematically. Yellow and white boxes represent *sltA* coding and flanking regions, respectively. The construct did not include any selection marker because thiamine-responding *sltA* clones were directly selected for Na^+ tolerance. (**B**) New mutations in *sltA*. Nucleotide numbering starts from the A in the initiation codon of the genomic *sltA* sequence (AN2919). *fs*, frame shift; *ins*, insertion, * indicates a stop codon. *sltA* encodes a 698-residue protein with three zinc fingers within residues 414–500.

Conditional suppression of ESCRT *vpsΔ* mutations by controlled downregulation of *sltA*

To facilitate manipulation of *vpsΔ* strains in both suppressed and unsuppressed states, we replaced by homologous recombination the endogenous promoter of the *sltA* gene by the regulatable *thiA* (thiazole synthase, AN3928) promoter. The resulting conditional allele was denoted *thiA^p::sltA*. The *thiA* promoter is shut off in the presence of low concentrations (at least 100 nM) of thiamine, and thus it is ideally suited for the manipulation of *sltA* because the shift between permissive and restrictive *sltA* expression conditions does not involve major changes in growth temperature, nitrogen or carbon source that might alter the physiology of the cells. We used this conditional allele extensively for subcellular studies after confirming that *thiA^p::sltA* strains grow very poorly on thiamine-containing medium containing 1 M NaH_2PO_4, thus largely resembling null *sltAΔ* and strong *sltA51* and *sltA58* loss-of-function mutants (Fig. 1A). By contrast, they are phenotypically wild-type for each and every aspect of *sltA* function that we tested in the absence of the vitamin (Fig. 1A; Fig. 2, compare line 1 with lines 19 and 20). The conditional *sltA* allele allowed study of the transition between the unsuppressed and suppressed *vpsΔ* states and, importantly, it also enabled propagation of unsuppressed *vpsΔ* strains by conidiospore transfer, as mutant conidiospores can be obtained from cultures grown in the presence of thiamine (i.e. phenotypically *sltA*$^-$) and germinated in the absence of thiamine (*sltA*$^+$ conditions) to establish their terminal phenotypes.

Different degrees of suppression of ESCRT null mutations by SltA downregulation

To compare suppressed and unsuppressed *vpsΔ* strains in completely isogenic backgrounds, *thiA^p::sltA* was introduced by crossing into *vpsΔ* strains, replacing the spontaneous (*slt*) suppressor mutations. On solid medium at 37℃ (the standard *A. nidulans* growth temperature), *vps27Δ*, *vps23Δ*, *vps36Δ*, *vps20Δ* and *vps32Δ* strains grew very poorly without thiamine (i.e. under *sltA*$^+$ conditions), in agreement with the conclusion that the genes are nearly essential (Fig. 2, lines 5, 7, 9, 11 and 13). Addition of thiamine permitted growth to different extents depending on the ESCRT gene, with *vps27Δ* showing the strongest and *vps32Δ* the weakest suppression (Fig. 2, lines 5, 7, 9, 11 and 13). These data indicate that not every ESCRT null allele is equally suppressible by *sltA* downregulation. Vps32 is the key structural component of ESCRT polymers (Babst et al., 1998; Saksena et al., 2009; Teis et al., 2008; Teis et al., 2010; Wollert et al., 2009; Wollert and Hurley, 2010) and thus it is not unexpected that its absence compromises viability to a greater extent than the absence of other ESCRT proteins. For example, in *Yarrowia lipolytica*, deletion of *VPS32* is lethal whereas inactivation of *VPS23* or *VPS28* is not (Blanchin-Roland et al., 2005). The crucial role of *A. nidulans* Vps32 was further confirmed by replacing the endogenous *vps32* promoter by the ethanol-inducible and glucose-repressible *alcA^p* (McGoldrick et al., 1995). Transformants confirmed to carry the expected gene replacement by Southern analysis (data not shown), were able to grow on ethanol and unable to grow on glucose, in agreement with the contention that Vps32 is virtually essential (supplementary material Fig. S2).

Importantly, although suppression of *vps32Δ* by thiamine-repressed *thiA^p::sltA* was incomplete, we found that the *sltA54* allele consistently suppressed the *vps32Δ* growth defect to a greater extent (Fig. 2, lines 4 and 5). *sltA54* is a partial loss-of-function mutation that (unlike *sltA51*, *sltA58* and thiamine-repressed *thiA^p::sltA* strong loss-of-function alleles) impairs growth on 1 M NaH_2PO_4 only very weakly (Fig. 1) and allows some growth at pH 8 (Fig. 2, line 14). This finding establishes that *vps32Δ* suppression does not require the almost complete lack of *sltA* function, a conclusion that is buttressed by the fact that *sltA59*, which shows stronger growth on 1 M NaH_2PO_4 medium than repressed *thiA^p::sltA* (Fig. 1A), leads to the same degree of *vps27Δ* suppression as the latter (Fig. 2, lines 12 and 13). Data below and not shown established that partial loss-of-function *sltA* and *sltB* mutations strongly suppress *vps20Δ* and *vps24Δ*. All these findings indicate that the lack of requirement for complete loss of *sltA* function for *vpsΔ* suppression is general.

Terminal phenotypes of *vpsΔ* mutant strains

We next examined under the microscope the germination of *vpsΔ* conidiospores, which revealed that *vpsΔ* mutants show a clear growth defect exacerbated by high temperature. In the wild-type, conidiospores undergo isotropic growth during the initial hours of germination before establishing a polarity axis and emitting a germ-tube, which grows by apical extension. When *thiA^p::sltA* conidia were germinated under non-suppressing (i.e. without

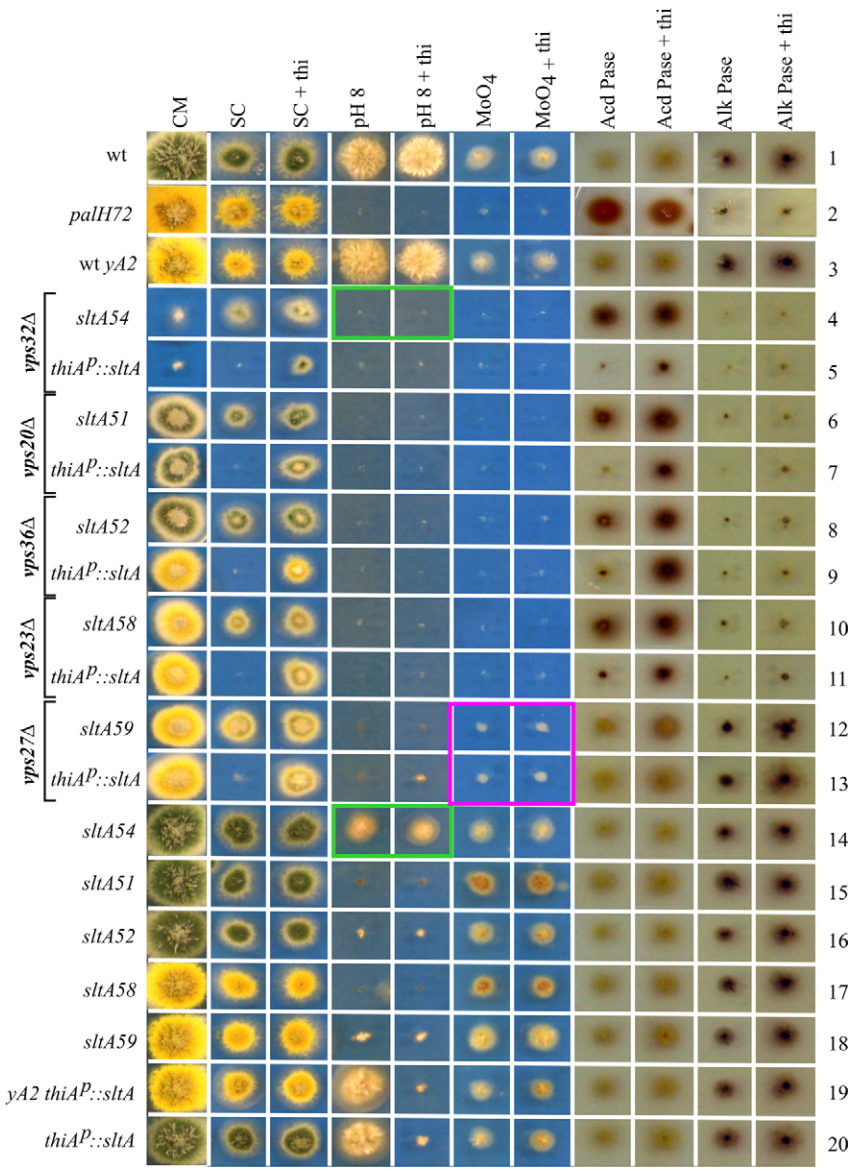

Fig. 2. Growth phenotypes of *vpsΔ* alleles in combination with classical *sltA*$^{-}$ alleles and with *thiA*^{p}*::sltA*. Strains were cultured on media diagnostic for pH regulation. CM, complete medium; SC, synthetic complete medium; thi, thiamine; pH 8, pH 8.0 SC medium; MoO_4, medium containing 33 mM sodium molybdate; Acd Pase and Alk Pase, extracellular acid and alkaline phosphatase staining, respectively. CM, which contains thiamine, supports better growth of *A. nidulans* strains than SC, including growth of suppressed *vpsΔ* strains excepting *vps32Δ*. The reason(s) why *vps32Δ thiA*^{p}*::sltA* and *vps32Δ sltA54* double mutant strains grow poorly on CM is unknown.

thiamine) conditions at 37℃, under which polarity establishment and maintenance were normal in *thiA*^{p}*::sltA* single mutant cells, *vps27Δ*, *vps23Δ*, *vps36Δ*, *vps20Δ* and *vps32Δ* strains were able to germinate and establish a polarity axis but they grew very slowly and showed morphological abnormalities such as swollen tips, abnormally high frequencies of septation and larger hyphal diameters (Fig. 3A; quantitative data are shown in supplementary material Fig. S3). The mutant apical extension rate was very slow at 37℃ but slightly higher at 25–27℃, allowing us to determine with confidence actual rates of apical extension from time-lapse sequences of Nomarski images (Fig. 3B). In *vps23Δ*, *vps36Δ* and *vps20Δ* strains, apical extension rate was reduced by ∽75% at 27℃, whereas in agreement with plate tests, the impairment in apical extension was somewhat less severe for *vps27Δ* hyphae. Unexpectedly, in *vps32Δ* cells the defect in apical extension was less severe than in *vps23Δ*, *vps36Δ* or *vps20Δ* cells (Fig. 3B, left panel). We feared that the incomplete degree of *vps32Δ* suppression by repressed *thiA*^{p}*::sltA* had led to selection of additional second-site suppressors during propagation of *thiA*^{p}*::sltA vps32Δ* colonies (see also supplementary material Fig. S3). Thus, for many experiments we used *sltA54* rather than *thiA*^{p}*::sltA* as a better suppressor of *vps32Δ*.

Under suppressing conditions (i.e. plus thiamine) all mutant strains grew similarly to the wild-type, with the exception of *vps27Δ* that, for reasons not evident, showed a significant increase in apical extension (Fig. 3B) ($P<0.001$; Turkey's multiple comparison test).

Diagnostic growth tests of pH regulation in ESCRT mutant strains

We determined the phenotypes of ESCRT null mutants in combination with *thiA*^{p}*::sltA* in diagnostic growth tests of pH regulation. These phenotypes were fully consistent with those of *vpsΔ* strains carrying classical *sltA*$^{-}$ mutations. Mutations preventing ambient pH signalling result in an acidity-mimicking phenotype, including failure to grow on pH 8 medium, hypersensitivity to molybdate toxicity, reduced staining for alkaline phosphatase and enhanced staining for

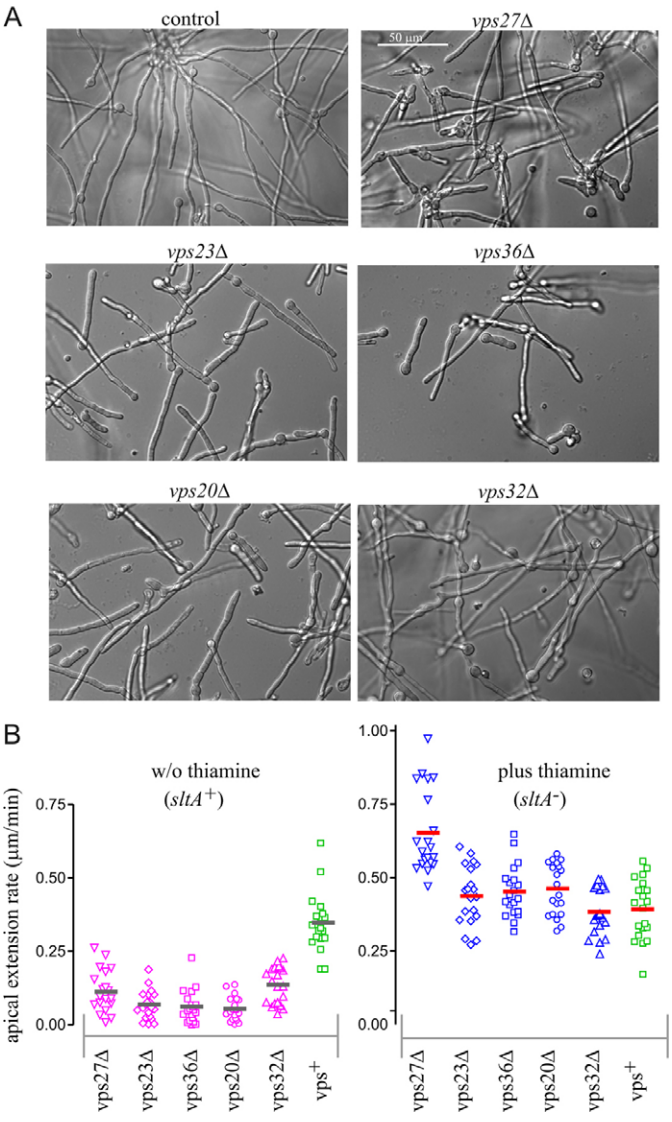

Fig. 3. Terminal phenotypes of ESCRT-deleted strains under non-suppressing conditions. (**A**) Conidiospore cultures were incubated overnight at 37℃ in synthetic complete medium lacking thiamine (*sltA*$^{+}$ conditions). (**B**) Apical extension rate for the indicated strains carrying ESCRT deletions in combination with *thiA*^{p}*::sltA* was determined in the presence and absence of thiamine. Horizontal bars show average of 20 determinations.

acid phosphatase (Caddick et al., 1986; Peñalva and Arst, 2002). Compare a *palH72* strain, carrying a null mutation in the ambient pH receptor gene, with wild-type strains (Fig. 2, lines 1–3).

SltA is necessary for growth on pH 8 medium (Spielvogel et al., 2008). Thus pH 8 medium cannot be used as a diagnostic test for an acidity-mimicking phenotype in the presence of loss-of-function *sltA*$^{-}$ mutations (Fig. 2, lines 15–18), an exception being the weak *sltA54* allele (Fig. 2, line 14). In the case of *thiA*^{p}*::sltA* strains, pH 8 medium cannot be used under thiamine-repressed conditions (Fig. 2, lines 19 and 20). However, the relative resistance of the weak *sltA54* allele to pH 8 allowed us to establish that *vps32Δ*, with which *sltA54* was isolated, leads to alkaline pH sensitivity (Fig. 2, compare lines 4 and 14, boxed in green).

Despite the fact that even when suppressed by loss-of-function *sltA* alleles, *vpsΔ* mutations generally reduce growth on minimal medium detectably, it is clear that *vps23Δ*, *vps36Δ*, *vps20Δ* and *vps32Δ* all result in molybdate hypersensitivity, markedly increased acid phosphatase staining and markedly decreased alkaline phosphatase staining (Fig. 2, lines 4–11, compare with the corresponding single mutant *sltA*$^{-}$ controls, lines 14–18, or with *thiA*^{p}*::sltA* controls, lines 19 and 20). We thus conclude that *vps23Δ*, *vps36Δ vps20Δ* and *vps32Δ* all result in an acidity-mimicking phenotype when their growth defects are suppressed by mutation of *sltA*. An important conclusion of these diagnostic tests was that *vps27Δ*, which is exceptional in that it virtually does not affect colony growth in the suppressed state, does not show any consistent acidity-mimicking phenotype (Fig. 2, lines 12 and 13). A slight effect on molybdate toxicity might be no more than a reflection of involvement of vacuolar biogenesis in molybdate tolerance. The pH signalling phenotype of the mutants will be further considered below.

ESCRT gene deletions result in numerous small vacuoles, which is remedied by *sltA*$^{-}$

As *sltA*$^{-}$ suppressing mutations result in hypervacuolation (Findon et al., 2010), we hypothesized that the key role(s) played by *Aspergillus* ESCRT genes is related to vacuolar function. Therefore, we examined vacuoles of *vpsΔ* mutants cultured under *sltA*$^{+}$ conditions, using a GFP-tagged version of PepA^{Pep12} (the only syntaxin present throughout the *A. nidulans* endocytic pathway) to label the vacuolar membranes. As in the wild-type (Findon et al., 2010), GFP–PepA^{Pep12} predominates in the vacuolar membranes of *thiA*^{p}*::sltA* single mutants cultured without thiamine (*sltA*$^{+}$ conditions). In marked contrast, GFP–PepA^{Pep12} labels abnormal aggregates of endomembranes in unsuppressed ESCRT null mutants. After inspecting deconvolved z-stacks and aided by CMAC co-staining, we concluded that these aggregates represent clusters of very small vacuoles. This ‘small vacuole phenotype’ was more extreme as the incubation temperature was raised (Fig. 4 shows representative examples, *vps23Δ* at 25℃ and *vps32Δ* at 37℃). z-stacks showed that these small vacuoles appear to be connected by tubular extensions (supplementary material Movies 1–3). Thus, these data strongly indicate that *vpsΔ* mutations result in ‘fragmented’ vacuoles (i.e. numerous small vacuoles).

We next addressed whether *vpsΔ* suppression by *sltA*$^{-}$ conditions involves remediation of this vacuolar phenotype. We used *thiA*^{p}*::sltA vpsΔ* cells cultured at 25℃ because at this temperature we could clearly resolve clusters of small vacuoles in the mutants cultured under non-suppressing (*sltA*$^{+}$) conditions. Fig. 5 shows representative examples for each of the *vpsΔ thiA*^{p}*::sltA* double mutant strains (*vps27Δ*, *vps23Δ*, *vps36Δ*, *vps20Δ* and *vps32Δ*), from cells cultured under *sltA*$^{-}$ and *sltA*$^{+}$ conditions. The numerous small vacuoles seen under *sltA*$^{+}$ conditions were never seen in cells cultured with thiamine (thus *sltA*$^{-}$). We conclude that loss of *sltA* function suppresses the ‘numerous small vacuoles’ phenotype resulting from ESCRT null mutations.

Null mutations in ESCRTs prevent trafficking of FM4-64 to vacuolar membranes

Suppression of the ‘numerous small vacuoles’ phenotype of *vpsΔ* mutants by *sltA*$^{-}$ conditions allowed us to test whether FM4-64 reaches the membrane of *vpsΔ* vacuoles. The endocytic tracer FM4-64 labels strongly the wild-type *A. nidulans* mitochondria in addition to the vacuoles (Peñalva, 2005), somewhat hindering the visualisation of the latter. By contrast, vacuolar membrane staining

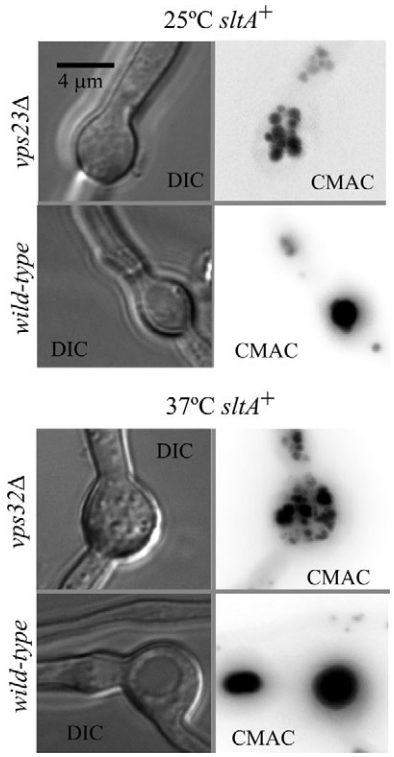

Fig. 4. Vacuolar phenotype in unsuppressed ESCRT mutants. Double mutant strains carrying *vps23Δ* or *vps32Δ*, in addition to *thiA*^{P}*::sltA* were cultured without thiamine (*sltA*$^{+}$ conditions) and loaded with CMAC. Images represent maximal intensity projections of deconvolved z-stacks (see supplementary material Movies 1–3).

with FM4-64 is very conspicuous in *sltA*$^{-}$ loss-of-function mutants and in *thiA*^{P}*::sltA* strains cultured under repressing conditions (Figs 6, 7; supplementary material Movie 4).

We tested, at 27℃, the effect of *vps32Δ* in a *sltA54* background (to avoid problems caused by incomplete suppression by the repressed *thiA*^{P}*::sltA* condition) (Fig. 6) and of *vps27Δ*, *vps23Δ*, *vps36Δ* and *vps20Δ* in a repressed *thiA*^{P}*::sltA* background (Fig. 7). All five *vpsΔ* mutations largely prevented traffic of FM4-64 to the vacuolar membranes, despite the fact that CMAC-stained vacuoles were nearly as prominent in the double mutants as in the single *sltA*$^{-}$ mutants (Figs 6, 7). In *S. cerevisiae*, ESCRT class E mutants display large multilamellar aggregates of endosomal membranes adjacent to the vacuoles (Raymond et al., 1992; Rieder et al., 1996), which are brightly stained by the endocytic tracer FM4-64. No conspicuous FM4-64-stainable compartments resembling vacuole-associated, *S. cerevisiae*-like class E compartments were noticeable in *sltA*$^{-}$ *vpsΔ* cells over the background of stained mitochondria.

Null mutations in ESCRTs prevent sorting to the vacuolar lumen of the endocytic cargo AgtA

We next investigated whether *vpsΔ* alleles prevent the MVB sorting of cargo destined to the vacuole using GFP-tagged dicarboxylic amino acid plasma membrane transporter AgtA, a prototypical cargo of the endocytic degradative pathway.

agtA is expressed in glutamate medium and is repressed very efficiently by ammonium (Apostolaki et al., 2009). Ammonium additionally regulates AgtA post-translationally, promoting the internalisation and MVB sorting of plasma membrane-resident AgtA. In pulse–chase experiments, cells cultured in glutamate are shifted to ammonium, and the fate of the permease determined by

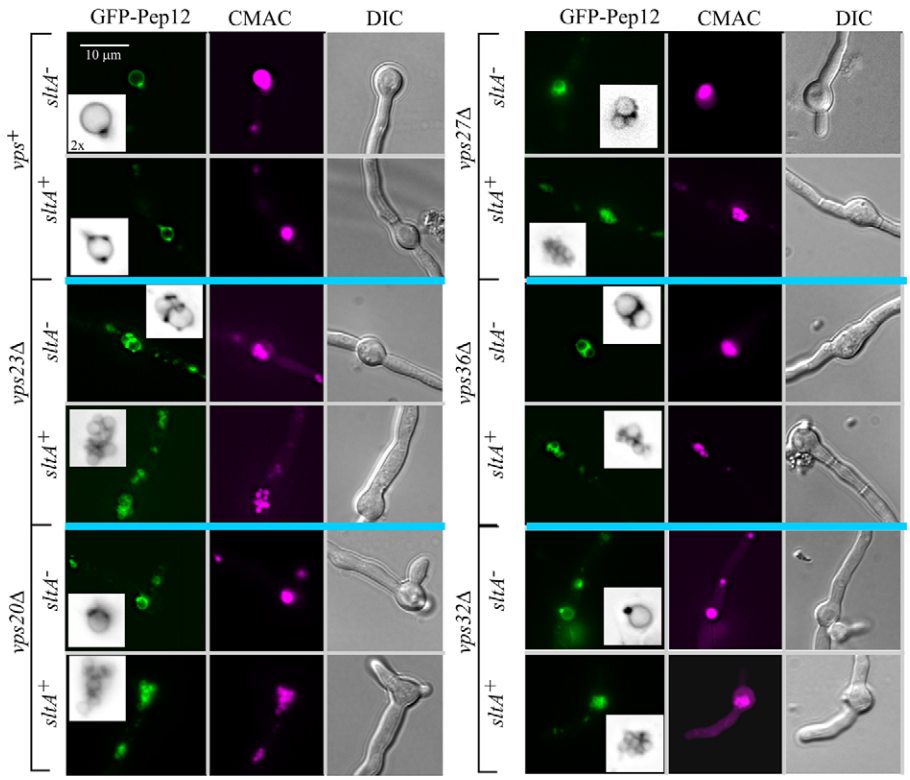

Fig. 5. Suppression of the ESCRT vacuolar phenotype by *sltA* inactivation. *thiA*^{P}*::sltA vpsΔ* double mutant cells expressing GFP–PepA^{Pep12} (GFP-Pep12) to visualise the vacuolar membrane were cultured at 27℃ in the presence or absence of thiamine and were loaded with CMAC to visualise the vacuolar lumen. All images are shown at the same magnification, with inverted contrast images (insets), corresponding to the GFP channel, shown at double magnification to facilitate visualisation of vacuoles.

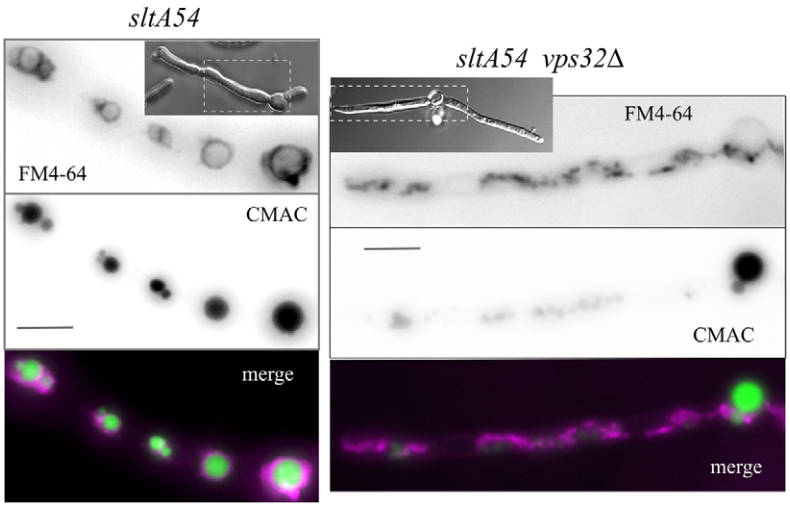

Fig. 6. Trafficking of FM4-64 to the vacuolar membrane is largely prevented by *vps32Δ*. *sltA54* cells, with or without *vps32Δ*, cultured at 27°C were loaded with FM4-64 and CMAC before being photographed. Insets show DIC images; dashed rectangles show regions of interest. All images are at the same magnification. Scale bars: 5 μm.

epifluorescence microscopy (Abenza et al., 2009; Abenza et al., 2010; Apostolaki et al., 2009; Hervás-Aguilar et al., 2010b).

We compared double *vpsΔ thiA^{p}::sltA* strains with *thiA^{p}::sltA* controls, both cultured under *sltA*-repressing conditions, to facilitate detection of the vacuoles. In repressed *thiA^{p}::sltA* (thus *sltA^{-}*) control cells growing on glutamate, AgtA–GFP predominates in the plasma membrane. When these cells are shifted to medium containing ammonium, AgtA is efficiently endocytosed and sorted into the vacuolar lumen, in a manner indistinguishable from that of the wild-type (Fig. 8). The ESCRT-0 mutation *vps27Δ* does not have any effect on the plasma membrane levels of the permease in glutamate medium nor does it prevent its endocytic internalisation upon shifting cells to ammonium. However, *vps27Δ* completely prevents endocytosed AgtA–GFP from reaching the vacuolar lumen, even at time points where virtually all the fluorescence is in the vacuolar lumen of *vps27^{+}* cells (Fig. 8; supplementary material Fig. S4 shows the kinetics of AgtA–GFP internalisation after the shift to ammonium). Instead, AgtA–GFP accumulates in dots in the cytoplasm of *vps27Δ* cells. These dots are almost certainly endosomes, as they resemble the endosomal compartments in which endocytosed AgtA accumulates in cells lacking RabB (Abenza et al., 2010), the endosomal Rab that determines acquisition of PtdIns(3)*P* by maturing early endosomes. In addition, AgtA reaches the vacuolar membranes of *vps27Δ* cells at late time points of its internalisation (supplementary material Fig. S4), suggesting that *vps27Δ* endosomes, unable to sort the permease into intralumenal vesicles (thus containing AgtA–GFP in their membrane), can fuse with the vacuole, albeit inefficiently. The absence of *vps27Δ* vacuolar lumen fluorescence, the predominance of endocytosed AgtA–GFP in endosomal compartments and the faint vacuolar membrane staining demonstrate that *vps27Δ* prevents the MVB sorting of the permease.

Delivery of AgtA into the vacuolar lumen was equally prevented by the ESCRT mutations *vps23Δ*, *vps36Δ*, *vps20Δ*

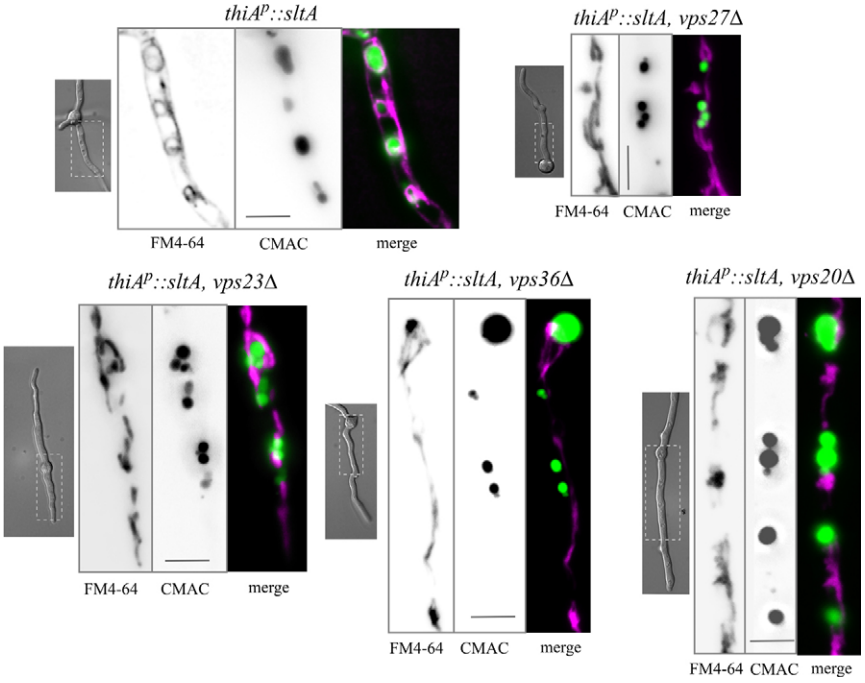

Fig. 7. Trafficking of FM4-64 to the vacuolar membrane is largely prevented by *vps27Δ*, *vps23Δ*, *vps36Δ* and *vps20Δ*. As for Fig. 6, but the cells were all additionally carrying *thiA^{p}::sltA*, rather than *sltA54*, and were cultured under thiamine (*sltA^{-}*) conditions. Scale bars: 5 μm.

Journal of Cell Science

Journal of Cell Science

and *vps32Δ*, resulting in AgtA accumulation in the vacuolar membranes, without detectable lumenal staining, after the ammonium shift (Fig. 8; data not shown for *vps23Δ* and *vps36Δ*). However, even though in ESCRT-I, ESCRT-II and ESCRT-III mutants AgtA was present in the plasma membrane during the incubation in glutamate medium, the fluorescent signal was very weak, and thus the reporter was most conspicuous in the membranes of septa (Fig. 8, arrowheads). These data strongly indicate that the ESCRT-I, ESCRT-II and ESCRT-III subunits tested play physiological roles beyond those of Vps27, and suggest that the former but not the latter are important for the presence (i.e. synthesis, delivery or turnover) of AgtA at the plasma membrane.

We conclude that all tested ESCRT genes are required for the MVB sorting of an endocytic cargo, although null *vps27Δ* (ESCRT-0) mutants phenotypically differ from the remaining ESCRT *vpsΔ* mutants in the compartment where they accumulate the endocytic permease (mainly endosomes in *vps27Δ* and vacuolar membranes in other ESCRT mutants).

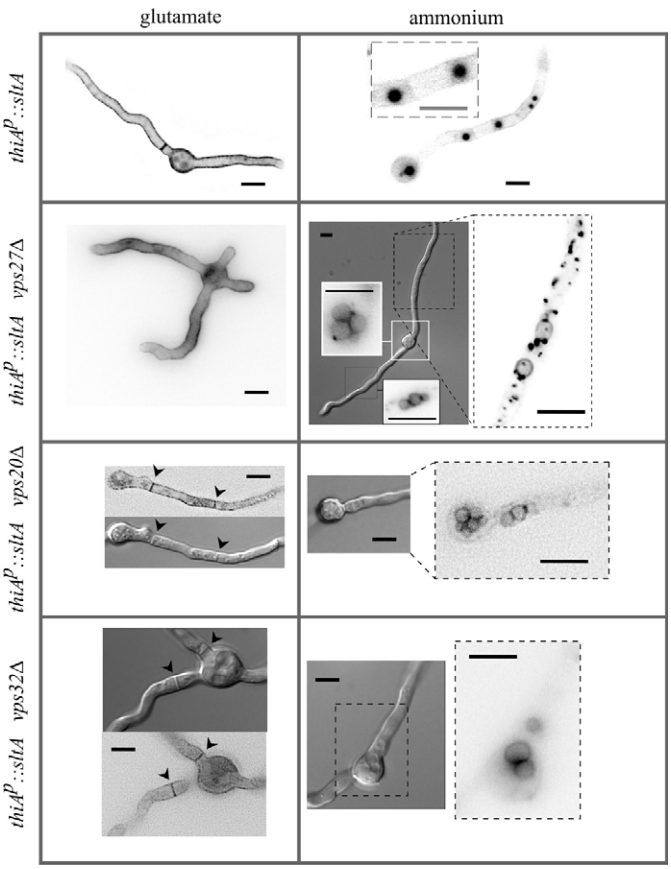

Fig. 8. Mis-sorting of endocytosed plasma membrane permease AgtA in ESCRT mutants. Cells expressing the plasma membrane transporter AgtA–GFP were cultured on synthetic complete medium containing thiamine, with glutamate as sole N source and then shifted to ammonium for 2 hours. Pictures were taken before (left) and after (right) the shift. Pictures in grey scale represent DIC images, whereas those in inverted contrast correspond to GFP fluorescence. Note the marked difference between *vps27Δ* and the ESCRT-III mutants shown (*vps20Δ* and *vps32Δ*). Arrowheads indicate septa (DIC) and membranes of septa (GFP). Scale bars: 5 μm.

Components of ESCRTs I, II and III, but not ESCRT-0, are required for pH signal transduction

At alkaline pH, signalling through the ambient pH signal transduction pathway results in the conversion of the full-length form PacC72 to PacC53, a committed intermediate and substrate for the pH-independent, proteasome-catalysed conversion to the fully processed and functional form PacC27 (Díez et al., 2002; Hervás-Aguilar et al., 2007). The growth-promoting effect that classical *sltA*$^{-}$ mutations have on the otherwise severely debilitated strains carrying ESCRT gene mutations allowed us to study the effect of the latter on the PacC proteolytic processing activation. We first determined, using pH shift experiments, that impairment of *sltA* or *sltB* function suppressing the growth *vpsΔ* phenotypes does not result in any noticeable changes in the pattern of PacC processing relative to a *sltA*$^{+}$ strain (Fig. 9, compare left and middle panels). Next, we examined PacC processing in cells carrying ESCRT null mutations in the *sltA*$^{-}$ or *sltB*$^{-}$ backgrounds, and compared the double mutant processing pattern with that of the corresponding *slt* single mutant. These experiments showed that lack of ESCRT-I Vps23, ESCRT-II Vps36 or ESCRT-III Vps20 or Vps32 prevents PacC processing. Thus, in terms of pH signalling activation, the consequences of the absence of ESCRT-I, ESCRT-II and ESCRT-III are essentially indistinguishable from those resulting from absence of PalH, PalF, PalC, PalA or PalB, all key dedicated components of the ambient pH signalling pathway.

Notably, and as reported for Rim101p processing in *S. cerevisiae* (Xu et al., 2004), the lack of ESCRT-0 Vps27 had no effect (Fig. 9, upper right panel). Thus, data for *vps27Δ* are consistent with growth tests described above (Fig. 2) and strongly indicate that the pH signalling defect seen in other ESCRT null mutants does not simply result from their inability to sort membrane and protein cargoes into the MVB pathway, as *vps27Δ* (*sltA59*) mutants are completely deficient in the sorting of cargoes to the vacuolar lumen.

Although unlikely, it is formally possible that abnormal accumulation of cargo in vacuolar membranes could indirectly lead to the pH signalling defect seen in *vps23Δ*, *vps36Δ*, *vps20Δ* and *vps32Δ* cells. Possibly arguing against this interpretation is the fact that *vps23Δ*, *vps36Δ* and *vps20Δ* are recessive in heterozygous diploids in diagnostic growth tests of pH regulation (supplementary material Fig. S5). *vps20Δ* and *vps36Δ* are also recessive with regard to AgtA–GFP trafficking to the vacuole in heterozygous diploids (supplementary material Fig. S5), indicating that the deletions do not have dominant-negative effects. Effects on pH regulation and AgtA trafficking might be expected if *vps*$^{+}$ alleles are haplo-insufficient.

The phospholipid PtdIns(3)*P* is a landmark of degradative endosomes undergoing maturation into multivesicular endosomes. Through its FYVE domain, Vps27 recognises endosomal domains and recruits ESCRT-I, ESCRT-II and ESCRT-III to them. Thus, the absence of involvement of Vps27 strongly indicates that pH signalling does not require degradative endosomes. *A. nidulans rabBΔ* mutants lack the Rab5 GTPase that determines degradative endosomal identity by recruiting the phosphoinositide 3-kinase Vps34 to endosomes (Abenza et al., 2010). In agreement with the above conclusion for *vps27Δ*, single *rabBΔ* mutant cells are indistinguishable from the wild-type in the alkaline pH-dependent processing of PacC (Fig. 10).

A. nidulans Vps24 is involved in the recruitment of the PalB protease to ESCRT-III-containing pH signalling complexes, at

Journal of Cell Science

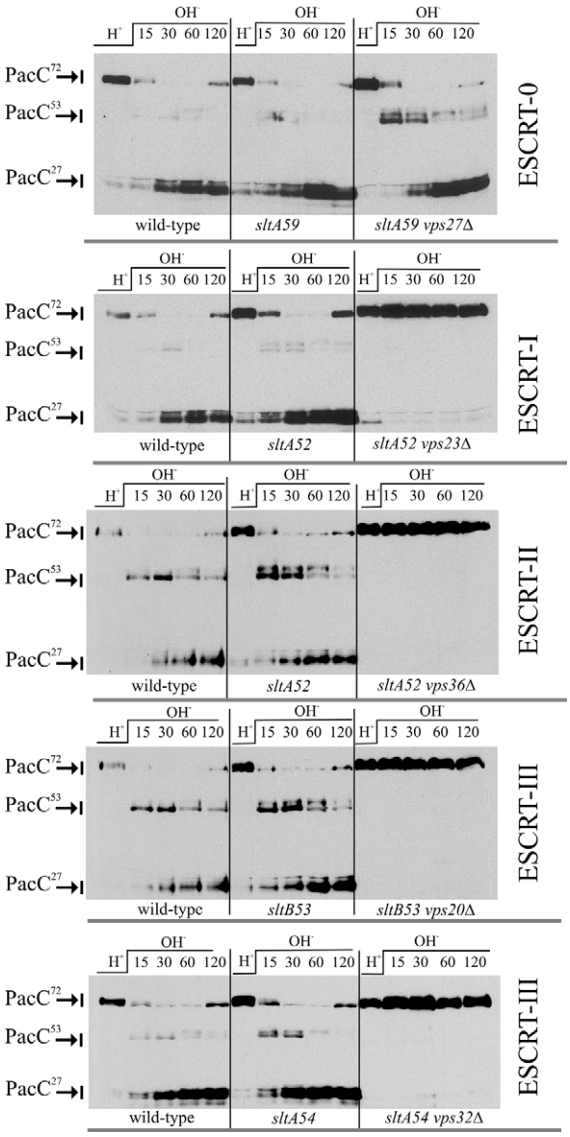

Fig. 9. Proteolytic processing activation of PacC prevented by ESCRT-I, ESCRT-II and ESCRT-III mutants, but not by *vps27Δ*. These experiments made use of classical *sltA*$^{-}$ and *sltB*$^{-}$ alleles. Wild-type, single *slt*$^{-}$ and double mutant *slt*$^{-}$ *vpsΔ* cells carrying *pacC900*, encoding Myc_3-PacC, were cultured under acidic pH conditions and shifted to alkaline conditions. Samples were taken at the indicated time points (after 15–120 minutes) and analysed by anti-Myc western blotting.

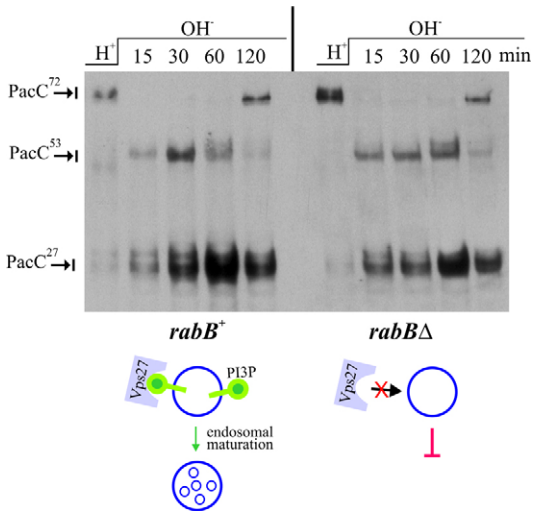

Fig. 10. Lack of effect of *rabBΔ* on the proteolytic processing activation of PacC. Anti-Myc western blotting was carried out as for Fig. 9. *rabBΔ* prevents the synthesis of PtdIns(3)*P* (green lollypops) on early endosomes and thus precludes Vps27 recruitment and subsequent ESCRT-mediated endosomal maturation. *rabBΔ* has no effect in the proteolytic processing activation of PacC.

least partly because the N-terminal MIT domain of PalB interacts directly with Vps24 (Rodríguez-Galán et al., 2009). Experiments with the human PalB orthologue calpain 7 have demonstrated that its MIT-mediated interaction with the ESCRT-III-associated protein IST1 stimulates its proteolytic activity (Osako et al., 2010). These data are consistent with a model in which recruitment of PalB to ESCRT-III activates the signalling protease. However, *S. cerevisiae vps24Δ* does not impair processing of Rim101p (Hayashi et al., 2005; Xu et al., 2004), in agreement with the fact that Rim13p does not have a MIT domain and that it appears to be recruited to ESCRT-III by Vps32p (Uetz et al., 2000). Deletion of the PalB MIT domain slows, but does not abolish, PacC proteolytic processing (Rodríguez-Galán et al., 2009), suggesting that other ESCRT-III proteins or a second, MIT-independent interaction with Vps24 might contribute to PalB recruitment to ESCRT-III. To address this key issue, we constructed vigorous *vps24Δ* mutants in a *sltA60* background [*sltA60* by itself does not have any effect on PacC processing (supplementary material Fig. S6)]. Fig. 11A,B shows that *vps24Δ* significantly impaired PacC signalling proteolysis (i.e. the alkaline pH-dependent conversion of PacC72 into PacC53), as indicated first by the persistently high levels of PacC72 detected upon shifting *vps24Δ* cells to alkaline conditions (Fig. 11B, top panel); and second by the corresponding lack of alkaline pH-dependent increase in the PacC53 pool seen in *vps24Δ* relative to controls (Fig. 11B, middle panel). Note that both in wild-type and single *sltA60* mutant cells, PacC72 is almost completely processed to PacC53 (and a proportion of PacC53 to PacC27) within 30 minutes (Fig. 11B, top panel; supplementary material Fig. S6).

However, contrasting with other ESCRT-III mutants, overall PacC processing to PacC27 can occur in *vps24Δ*, as shown by the high, yet seemingly invariable steady-state level of the proteolytic cascade product PacC27 detected throughout the pH shift (Fig. 11B, bottom panel), thus demonstrating that PacC processing can take place in the absence of Vps24. The facts that a considerable PacC27 pool exists in the *vps24Δ* mutant under acidic conditions (Fig. 11B, bottom panel, arrow), whereas no PacC27 is seen in controls; that this pool does not substantially increase upon shifting cells to alkaline pH (Fig. 11B, bottom panel); and that detectable ambient pH-independent conversion of PacC72 into PacC53 takes place in *vps24Δ* cells where PacC53 is detectable even under acidic conditions (Fig. 11B, middle panel, arrow) [under which virtually no PacC53 (i.e. no signalling cleavage) occurs in the wild-type or in single *sltA* mutants (Fig. 9, Fig. 11B, middle panel; supplementary material Fig. S6)] strongly indicate that, in addition to impairing the normal processing of PacC72, *vps24Δ* results in some

Journal of Cell Science

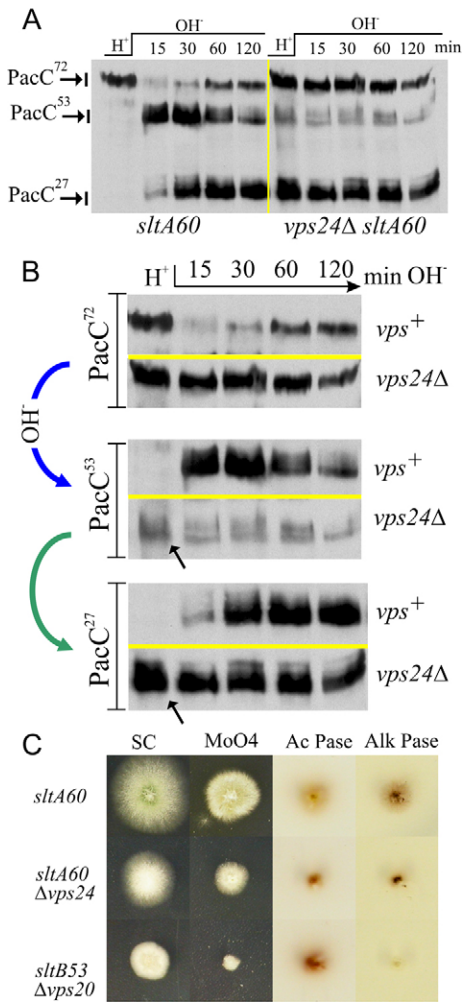

Fig. 11. Inefficient but pH-independent PacC processing activation in *vps24Δ* cells. (**A**) Western blot of an alkaline pH shift experiment showing the pattern of PacC processing in *vps24Δ sltA60* cells in comparison with that of *sltA60*, which is indistinguishable from the wild-type (see supplementary material Fig. S6). (**B**) Different regions of the western blot shown in A, aligned to enable direct comparison of how PacC72, PacC53 and PacC27 levels change across the pH shift in the *vps24Δ* mutant and its *vps*$^{+}$*sltA60* control. (**C**) Diagnostic tests of pH regulation show that, in contrast to *vps20Δ*, *vps24Δ* results in a weak acidity-mimicking phenotype. Media abbreviations as in Fig. 2.

pH-independent activation of the cascade. However inefficient, this pH-independent conversion of PacC72 into PacC53 resulting from *vps24Δ* suffices to build up a pool of the stable PacC27 product under acidic conditions.

These results establish that *vps24Δ* promotes a certain degree of processing under inappropriate conditions, a finding that agrees with the report that *S. cerevisiae vps24Δ* results in a small, yet detectable, degree of constitutivity (Hayashi et al., 2005) (see Discussion). We used diagnostic growth tests for pH regulation to reinforce this conclusion (Fig. 11C). These tests clearly showed that *vps24Δ* does not result in the extreme sensitivity to molybdate seen in *vps20Δ*, used here as control (as shown, *vps20Δ* fully prevents the proteolytic processing activation of PacC, and mutations impairing pH signalling result in hypersensitivity to molybdate; Fig. 2). Notably, *vps24Δ* allows substantial expression of alkaline phosphatase compared to *vps20Δ* and only slightly increased acid phosphatase levels compared to the wild-type, demonstrating that, in contrast to *vps20Δ*, *vps24Δ* results in only a weak acidity-mimicking phenotype, in agreement with the PacC processing experiments.

Discussion

We established that, unlike in yeasts such as *S. cerevisiae* and *Schizosaccharomyces pombe* (Iwaki et al., 2007), null mutations affecting *A. nidulans* ESCRT-0, ESCRT-I, ESCRT-II and ESCRT-III components are severely debilitating, extending our preliminary observation with Vps24 (Rodríguez-Galán et al., 2009). This severely debilitating phenotype has been a major hurdle for investigation of the roles of ESCRTs in *A. nidulans* pH signalling, a hurdle that we now clear by showing that inactivation of a fungal-specific salt-tolerance pathway rescues the severely debilitating effect resulting from the absence of Vps27, Vps23, Vps36, Vps20, Vps32 or Vps24. Not every null *vps* deletion is equally suppressible, with *vps27Δ* being the most and *vps32Δ* being the least suppressible, which agrees with the key role attributed to Vps32 in the formation of intraluminal vesicles in endosomes (Hierro et al., 2004; Saksena et al., 2009; Teis et al., 2008; Teis et al., 2010; Wollert et al., 2009; Wollert and Hurley, 2010).

In *S. cerevisiae*, ESCRT class E mutants display a large multilamellar aggregate of endosomal membranes adjacent to otherwise normally sized vacuoles (Raymond et al., 1992; Rieder et al., 1996). No such conspicuous compartment is observable in *A. nidulans* ESCRT mutants that, in the unsuppressed state, instead accumulate clusters of very small vacuoles, a defect that is exacerbated by high temperature. Suppression of the severely debilitating ESCRT null phenotype by *sltA*$^{-}$ correlates with recovery of normal-sized vacuoles, but the ESCRT phenotype cannot be solely attributed to the inability to form regularly sized vacuoles because *A. nidulans rab7Δ* mutants also show numerous small vacuoles but only a very minor growth defect (J.F.A. and M.A.P., unpublished results). Why inactivation of the SltA–SltB salt-tolerance pathway suppresses null ESCRT mutants is presently unknown. We chose to manipulate SltA because it is a zinc-finger, filamentous fungal-specific transcription factor, and thus almost certainly the ultimate mediator of this pathway. Its transcriptional domain is currently under investigation, but whichever are the structural genes whose expression is altered by inactivation of *sltA*, such inactivation clearly results in marked enlargement of the vacuolar system. This was established using FM4-64 and endovacuolar t-SNARE PepA^{Pep12} in classical and engineered *sltA*$^{-}$ mutant strains, as well as in phenotypically indistinguishable *sltB*$^{-}$ strains. It is worth noting that in *A. nidulans*, maturation of early endosomes into late endosomes is also essential (Abenza et al., 2010), and thus it is not unexpected that precluding MVB biogenesis (which is coupled to this maturation) is also severely debilitating. We speculate that the need of endosomal maturation for membrane and cargo delivery to vacuoles might be bypassed in *sltA* deficiency.

Studies pioneered by the Mitchell laboratory (Carnegie Mellon University, Pittsburgh, PA) established involvement of all components of ESCRT-I and ESCRT-II, and Vps20 and Vps32 of ESCRT-III, in the proteolytic activation of the yeast PacC orthologue Rim101p (Boysen et al., 2010; Boysen and Mitchell, 2006; Hayashi et al., 2005; Rothfels et al., 2005; Xu et al., 2004).

Journal of Cell Science

Our pH shift experiments established unambiguously that the absence of Vps23, Vps36, Vps20 or Vps32 prevents PacC processing. Direct involvement of at least Vps23 and Vps32 is unquestionable. Vps32 binds directly to two of the six pH signalling proteins, PalA and PalC. PalA is a specialised fungal version of Alix that, like the latter, efficiently binds YPXL/I motifs (Vincent et al., 2003). PalC is a Bro1 domain-like protein where substitutions impairing its interaction with Vps32 also impair pH signalling (Galindo et al., 2007; Tilburn et al., 2005). Vps23 binds the Rim8p (PalF homologue) arrestin (Herrador et al., 2009). PalF itself not only binds avidly the 7-TMD receptor PalH but is able to promote PalH localisation to the plasma membrane (Hervás-Aguilar et al., 2010a), adding to the increasing body of evidence supporting a model in which pH signalling complexes mediate ESCRT recruitment to the plasma membrane. Such evidence includes the key finding that the Vps32 interactor PalC, expressed at physiological levels, is recruited to cortical structures in a signalling-dependent manner (Galindo et al., 2007). Work in preparation (A.G., A.M.C.-P., H.N.A. and M.A.P.) has established that one component of ESCRT localises, in addition to endosomes, to cortical structures in an alkaline ambient pH- and *palF*-dependent manner.

In agreement with this view, we report here further evidence that endosomal ESCRTS are not required for pH signalling: *rabBΔ* mutants cannot recruit Vps27 to endosomes (Abenza et al., 2010), which would result in less efficient assembly of ESCRTs in these organelles. However, these mutants show normal PacC processing (Fig. 9). Indeed the Mitchell study (Xu et al., 2004) and this work show that Vps27 is fully dispensable for signalling in both *S. cerevisiae* and *A. nidulans*. Moreover, forced recruitment of Rim20p to endosomes does not promote Rim101p activation (Boysen et al., 2010), and the role played by Vps32 in pH signalling in yeasts can be mutationally separated from its role in the MVB pathway (Weiss et al., 2009; Wolf and Davis, 2010).

What is the factor(s) that can substitute ESCRT-0 at the plasma membrane? Herrador et al. (Herrador et al., 2009) have shown that one such factor is almost certainly the Rim8/PalF arrestin. The yeast Vps23p UEV domain binds a PTAP-related motif in Rim8p and, additionally, binds ubiquitin residues that Rsp5p adds onto Rim8p. These two interactions reinforce each other. Because PalF is ubiquitylated in an alkaline pH-dependent manner (Herranz et al., 2005), these data strongly support a model in which a conformational change in the receptor drives PalF ubiquitylation at the plasma membrane, which would promote the recruitment of Vps23 and thus other ESCRTs to plasma membrane pH signalling complexes visualised with PalC. In strong support, an artificially ubiquitylated version of PalF, expressed at physiological levels, results in 'true' (receptor-independent) constitutivity (Hervás-Aguilar et al., 2010a).

Vps24 deserves separate consideration because here the key point is how (and where) the calpain-like protease PalB/Rim13p is activated to mediate PacC/Rim101p processing. *S. cerevisiae vps24Δ* promotes some degree of activation of the pathway, but this activation is receptor-dependent, and therefore cannot be considered as truly constitutive. We demonstrate that, in *A. nidulans*, *vps24Δ* also results in some degree of pH-independent processing. As Vps24 is thought to terminate polymerisation of Vps32 in ESCRT-III (Teis et al., 2008; Wollert and Hurley, 2010), it is plausible that *vps24Δ* 'sensitises' the pathway by increasing the half-life and/or surface of Vps32 polymer available for pH signalling Vps32 interactors.

A. nidulans PalB contains a MIT domain binding Vps24. PalB MIT deletion impairs processing (Rodríguez-Galán et al., 2009), as does *vps24* deletion (this work) but neither mutation precludes PacC processing. It is plausible that other proteins like Vps32 [which binds Rim13p in *S. cerevisiae* (Ito et al., 2001)] contribute to recruiting PalB to signalling complexes. Moreover, it is also plausible that the MIT–Vps24 interaction regulates PalB, rather than (or in addition to) recruiting it to ESCRT-III: Maki's group (Nagoya University, Nagoya, Japan) recently demonstrated that the two MIT domains of calpain 7, the human PalB orthologue, interact with the two MIM motifs of the ESCRT-III-associated protein IST1 and, importantly, that this binding activates calpain 7, implying that the enzyme is activated by ESCRT-III. (Osako et al., 2010). Thus, the Vps24 MIM–PalB MIT interaction could similarly mediate the localised activation of PalB. This hypothetical scenario wherein recruitment to ESCRT activates PalB is consistent with the well-established fact that processing of the likely PalB substrate PacC involves binding, via two YPXL/I motifs in the transcription factor, to the Vps32 interactor PalA (Vincent et al., 2003; Xu and Mitchell, 2001).

Materials and Methods

A. nidulans techniques

Growth media (Cove, 1966) and *A. nidulans* genetic methodologies (Clutterbuck, 1993; Pontecorvo et al., 1953; Szewczyk et al., 2006) were as described. Strains (supplementary material Table S1) carried standard markers (Clutterbuck, 1993). Strain AMC56 was used for *vps* gene replacement by *A. fumigatus pyrG*. All transformed strains were confirmed for homologous integration and gene replacement by Southern and PCR analyses. pH regulatory phenotypes and pH shift experiments have been described (Caddick et al., 1986; Hervás-Aguilar et al., 2007; Tilburn et al., 1995). Na^+ sensitivity (Findon et al., 2010; Spielvogel et al., 2008) was tested using 1 M NaH_2PO_4. Protein extraction, SDS-PAGE and western blotting followed reported procedures (Hervás-Aguilar et al., 2007; Hervás-Aguilar and Peñalva, 2010).

Gene deletions and suppressors

Deletion cassettes for *vps27* (AN2071), *vps23* (AN2521), *vps36* (AN7037), *vps20* (AN1365), *vps32* (AN4240) and *vps24* (AN6920) were constructed by fusion PCR (Yu et al., 2004). Heterokaryotic primary transformants were analysed following the method of Osmani (Osmani et al. 2006). Phenotypes of *vps* deletions co-segregated with the deletion construct in progeny from meiotic crosses. *vpsΔ* and suppressor mutations segregated in each cross. Excepting *vps32Δ* crosses in which only suppressed *vps32Δ* progeny were obtained, both suppressed and unsuppressed *vpsΔ* progeny were recovered. *sltA* and *sltB* mutations were determined by sequencing (primers listed in supplementary material Table S2).

Construction of gene fusion alleles

The endogenous *sltA* promoter was replaced with the *A. nidulans thiA* (AN10492) promoter ($thiA^P$), following work in *Aspergillus oryzae* (Shoji et al., 2005). A linear $thiA^P$*::sltA* fragment driving expression of *sltA* under the control of $thiA^P$ was assembled by fusion PCR (Yu et al., 2004) and used to transform a *nkuAΔ::bar sltA1* strain (HHF26c; supplementary material Table S1). *sltA1* (O'Neil et al., 2002) is a nonsense mutation resulting in loss of the C-terminal region downstream of the zinc finger region and results in Na^+ toxicity. Gene-replaced transformants were selected on regeneration medium (Tilburn et al., 1983) containing 1 M NaH_2PO_4. One transformant having a single homologous integration was chosen for further work.

Microscopy

A. nidulans was cultured at 25℃, 27℃ or 37℃ in watch minimal medium (WMM) (Peñalva, 2005) using culture dishes (MatTek, Boston, MA) or eight-well chambers (Ibidi, Munich, Germany). Images were acquired using Improvision Volocity software and a Zeiss Axiovert 200 inverted microscope, housed within a controlled-temperature incubation chamber. Z-stacks were acquired using a 63 × 1.4 NA objective, a Hamamatsu ORCA-ER camera and Zeiss filter sets 10 (emission BP 515–565 nm) and 01 (emission LP 397 nm) for GFP and CMAC, respectively, and Semrock TxRed-4040B (emission BP 624/640 nm) for FM4-64. z-series stacks were deconvolved using Huygens software. Images were processed with Metamorph (Molecular Devices).

Staining with FM4-64 (5 μM in WMM) and CMAC (C2110, Molecular Probes, Invitrogen; 10 μM final concentration) followed the method of Peñalva (Peñalva,

Journal of Cell Science

2005), using cells cultured in WMM. At 5 minutes after loading FM4-64, the culture was washed with WMM and, after an additional 50 minutes of incubation, CMAC was loaded and washed with WMM before immediately examining cells by fluorescence microscopy. To determine apical extension rates, conidiospores were cultured in WMM at 27℃ for 15 hours without thiamine. To repress *sltA* expression, 100 μM (final concentration) of thiamine was added. Apical extension rates were determined after 5 hours of additional incubation, using Nomarski images taken every 10 minutes with a 10× objective.

Acknowledgements

We thank Claudio Scazzocchio for suggesting the use of the *thiA*^{p}, Martine Mathieu for the *thiA* promoter sequence, Patricia López-Calcagno for constructing the *thiA*^{p}::*sltA* allele, Tatiana Múnera-Huertas, Victoria Crome and Elena Reoyo for technical assistance and Martin Spitaler (FILM) for help with microscopy.

Funding

This work was supported by the Biotechnology and Biological Sciences Research Council [grant numbers BB/D521781/1 to H.N.A., BB/F01189X/1 to H.N.A. and Elaine Bignell]; the Wellcome Trust [grant numbers 067878, 084660/Z/08/Z to H.N.A. and Joan Tilburn]; the Spanish Government [grant number BIO2009-7281 to M.A.P.]; and Comunidad de Madrid [grant number SAL/0246/2006 to M.A.P.]. J.F.A. was a CSIC I3P fellow. Deposited in PMC for immediate release.

Supplementary material available online at
http://jcs.biologists.org/lookup/suppl/doi:10.1242/jcs.088344/-/DC1

References

Abenza, J. F., Pantazopoulou, A., Rodríguez, J. M., Galindo, A. and Peñalva, M. A. (2009). Long-distance movement of *Aspergillus nidulans* early endosomes on microtubule tracks. *Traffic* **10**, 57-75.

Abenza, J. F., Galindo, A., Pantazopoulou, A., Gil, C., de los Ríos, V. and Peñalva, M. A. (2010). *Aspergillus* RabB^{Rab5} integrates acquisition of degradative identity with the long-distance movement of early endosomes. *Mol. Biol. Cell* **21**, 2756-2769.

Apostolaki, A., Erpapazoglou, Z., Harispe, L., Billini, M., Kafasla, P., Kizis, D., Peñalva, M. A., Scazzocchio, C. and Sophianopoulou, V. (2009). AgtA, the dicarboxylic amino acid transporter of *Aspergillus nidulans*, is concertedly down-regulated by exquisite sensitivity to nitrogen metabolite repression and ammonium-elicited endocytosis. *Eukaryot. Cell* **8**, 339-352.

Babst, M., Wendland, B., Estepa, E. J. and Emr, S. D. (1998). The Vps4p AAA ATPase regulates membrane association of a Vps protein complex required for normal endosome function. *EMBO J.* **17**, 2982-2993.

Blanchin-Roland, S., Da Costa, G. and Gaillardin, C. (2005). ESCRT-I components of the endocytic machinery are required for Rim101-dependent ambient pH regulation in the yeast *Yarrowia lipolytica*. *Microbiology* **151**, 3627-3637.

Boysen, J. H. and Mitchell, A. P. (2006). Control of Bro1-domain protein Rim20 localization by external pH, ESCRT machinery, and the *Saccharomyces cerevisiae* Rim101 pathway. *Mol. Biol. Cell* **17**, 1344-1353.

Boysen, J. H., Subramanian, S. and Mitchell, A. P. (2010). Intervention of Bro1 in pH-responsive Rim20 localization in *Saccharomyces cerevisiae*. *Eukaryot. Cell* **9**, 532-538.

Caddick, M. X., Brownlee, A. G. and Arst, H. N., Jr (1986). Regulation of gene expression by pH of the growth medium in *Aspergillus nidulans*. *Mol. Gen. Genet.* **203**, 346-353.

Calcagno-Pizarelli, A. M., Negrete-Urtasun, S., Denison, S. H., Rudnicka, J. D., Bussink, H.-J., Munera-Huertas, T., Stanton, L., Hervás-Aguilar, A., Espeso, E. A., Tilburn, J. et al. (2007). Establishment of the ambient pH signaling complex in *Aspergillus nidulans*: PalI assists plasma membrane localization of PalH. *Eukaryot. Cell* **6**, 2365-2375.

Clutterbuck, A. J. (1993). *Aspergillus nidulans*. In *Genetic maps. Locus maps of complex genomes*, Vol. 3, (ed. S. J. O'Brien), pp. 3.71-3.84. Cold Spring Harbor: Cold Spring Harbor Laboratory Press.

Cornet, M., Bidard, F., Schwarz, P., Da Costa, G., Blanchin-Roland, S., Dromer, F. and Gaillardin, C. (2005). Deletions of endocytic components *VPS28* and *VPS32* affect growth at alkaline pH and virulence through both RIM101-dependent and RIM101-independent pathways in *Candida albicans*. *Infect. Immun.* **73**, 7977-7987.

Cove, D. J. (1966). The induction and repression of nitrate reductase in the fungus *Aspergillus nidulans*. *Biochim. Biophys. Acta* **113**, 51-56.

Díez, E., Álvaro, J., Espeso, E. A., Rainbow, L., Suárez, T., Tilburn, J., Arst, H. N., Jr and Peñalva, M. A. (2002). Activation of the *Aspergillus* PacC zinc-finger transcription factor requires two proteolytic steps. *EMBO J.* **21**, 1350-1359.

Findon, H., Calcagno-Pizarelli, A. M., Martínez, J. L., Spielvogel, A., Markina-Iñarrairaegui, A., Indrakumar, T., Ramos, J., Peñalva, M. A., Espeso, E. A. and Arst, H. N., Jr (2010). Analysis of a novel calcium auxotrophy in *Aspergillus nidulans*. *Fungal Genet. Biol.* **47**, 647-655.

Galindo, A., Hervás-Aguilar, A., Rodríguez-Galán, O., Vincent, O., Arst, H. N., Jr, Tilburn, J. and Peñalva, M. A. (2007). PalC, one of two Bro1 domain proteins in the fungal pH signaling pathway, localizes to cortical structures and binds Vps32. *Traffic* **8**, 1346-1364.

Hayashi, M., Fukuzawa, T., Sorimachi, H. and Maeda, T. (2005). Constitutive activation of the pH-responsive Rim101 pathway in yeast mutants defective in late steps of the MVB/ESCRT pathway. *Mol. Cell. Biol.* **25**, 9478-9490.

Herrador, A., Herranz, S., Lara, D. and Vincent, O. (2009). Recruitment of the ESCRT machinery to a putative seven-transmembrane-domain receptor is mediated by an arrestin-related protein. *Mol. Cell. Biol.* **30**, 897-907.

Herranz, S., Rodríguez, J. M., Bussink, H. J., Sánchez-Ferrero, J. C., Arst, H. N., Jr, Peñalva, M. A. and Vincent, O. (2005). Arrestin-related proteins mediate pH signaling in fungi. *Proc. Natl. Acad. Sci. USA* **102**, 12141-12146.

Hervás-Aguilar, A. and Peñalva, M. A. (2010). Endocytic machinery protein SlaB is dispensable for polarity establishment but necessary for polarity maintenance in hyphal tip cells of *Aspergillus nidulans*. *Eukaryot. Cell* **9**, 1504-1518.

Hervás-Aguilar, A., Rodríguez, J. M., Tilburn, J., Arst, H. N., Jr and Peñalva, M. A. (2007). Evidence for the direct involvement of the proteasome in the proteolytic processing of the *Aspergillus nidulans* zinc finger transcription factor PacC. *J. Biol. Chem.* **282**, 34735-34747.

Hervás-Aguilar, A., Galindo, A. and Peñalva, M. A. (2010a). Receptor-independent ambient pH signaling by ubiquitin attachment to fungal arrestin-like PalF. *J. Biol. Chem.* **285**, 18095-18102.

Hervás-Aguilar, A., Rodríguez-Galán, O., Galindo, A., Abenza, J. F., Arst, H. N., Jr and Peñalva, M. A. (2010b). Characterization of *Aspergillus nidulans* DidB^{Did2}, a non-essential component of the multivesicular body pathway. *Fungal Genet. Biol.* **47**, 636-646.

Hierro, A., Sun, J., Rusnak, A. S., Kim, J., Prag, G., Emr, S. D. and Hurley, J. H. (2004). Structure of the ESCRT-II endosomal trafficking complex. *Nature* **431**, 221-225.

Hurley, J. H. and Emr, S. D. (2006). The ESCRT complexes: structure and mechanism of a membrane-trafficking network. *Annu. Rev. Biophys. Biomol. Struct.* **35**, 277-298.

Hurley, J. H. and Hanson, P. I. (2010). Membrane budding and scission by the ESCRT machinery: it's all in the neck. *Nat. Rev. Mol. Cell. Biol.* **11**, 556-566.

Ito, T., Chiba, T., Ozawa, R., Yoshida, M., Hattori, M. and Sakaki, Y. (2001). A comprehensive two-hybrid analysis to explore the yeast protein interactome. *Proc. Natl. Acad. Sci. USA* **98**, 4569-4574.

Iwaki, T., Onishi, M., Ikeuchi, M., Kita, A., Sugiura, R., Giga-Hama, Y., Fukui, Y. and Takegawa, K. (2007). Essential roles of class E Vps proteins for sorting into multivesicular bodies in *Schizosaccharomyces pombe*. *Microbiology* **153**, 2753-2764.

Katzmann, D. J., Odorizzi, G. and Emr, S. D. (2002). Receptor downregulation and multivesicular-body sorting. *Nat. Rev. Mol. Cell Biol.* **3**, 893-905.

Kullas, A. L., Li, M. and Davis, D. A. (2004). Snf7p, a component of the ESCRT-III protein complex, is an upstream member of the RIM101 pathway in *Candida albicans*. *Eukaryot. Cell* **3**, 1609-1618.

Li, W. S. and Mitchell, A. P. (1997). Proteolytic activation of Rim1p, a positive regulator of yeast sporulation and invasive growth. *Genetics* **145**, 63-73.

McDonald, B. and Martin-Serrano, J. (2009). No strings attached: the ESCRT machinery in viral budding and cytokinesis. *J. Cell. Sci.* **122**, 2167-2177.

McGoldrick, C. A., Gruver, C. and May, G. S. (1995). *myoA* of *Aspergillus nidulans* encodes an essential myosin I required for secretion and polarized growth. *J. Cell Biol.* **128**, 577-587.

Mitchell, A. P. (2008). A VAST staging area for regulatory proteins. *Proc. Natl. Acad. Sci. USA* **105**, 7111-7112.

O'Neil, J. D., Bugno, M., Stanley, M. S., Barham-Morris, J. B., Woddcock, N. A., Clement, D. J., Clipson, N. J. W., Whitehead, M. P. and Fincham, D. A. H. P. (2002). Cloning of a novel gene encoding a C2H2 zinc finger protein that alleviates sensitivity to abiotic stresses in *Aspergillus nidulans*. *Mycol. Res.* **106**, 491-498.

Orejas, M., Espeso, E. A., Tilburn, J., Sarkar, S., Arst, H. N. Jr and Peñalva, M. A. (1995). Activation of the *Aspergillus* PacC transcription factor in response to alkaline ambient pH requires proteolysis of the carboxy-terminal moiety. *Genes Dev.* **9**, 1622-1632.

Osako, Y., Maemoto, Y., Tanaka, R., Suzuki, H., Shibata, H. and Maki, M. (2010). Autolytic activity of human calpain 7 is enhanced by ESCRT-III-related protein IST1 through MIT-MIM interaction. *FEBS J.* **277**, 4412-4426.

Osmani, A. H., Oakley, B. R. and Osmani, S. A. (2006). Identification and analysis of essential *Aspergillus nidulans* genes using the heterokaryon rescue technique. *Nat. Protoc.* **1**, 2517-2526.

Peñalva, M. A. (2005). Tracing the endocytic pathway of *Aspergillus nidulans* with FM4-64. *Fungal Genet. Biol.* **42**, 963-975.

Peñalva, M. A. and Arst, H. N., Jr (2002). Regulation of gene expression by ambient pH in filamentous fungi and yeasts. *Microbiol. Mol. Biol. Rev.* **66**, 426-446.

Peñalva, M. A. and Arst, H. N., Jr (2004). Recent advances in the characterization of ambient pH regulation of gene expression in filamentous fungi and yeasts. *Annu. Rev. Microbiol.* **58**, 425-451.

Peñalva, M. A., Tilburn, J., Bignell, E. and Arst, H. N., Jr (2008). Ambient pH gene regulation in fungi: making connections. *Trends Microbiol.* **16**, 291-300.

Peñas, M. M., Hervás-Aguilar, A., Múnera-Huertas, T., Reoyo, E., Peñalva, M. A., Arst, H. N., Jr and Tilburn, J. (2007). Further characterization of the signaling proteolysis step in the *Aspergillus nidulans* pH signal transduction pathway. *Eukaryot. Cell* **6**, 960-970.

Pontecorvo, G., Roper, J. A., Hemmons, L. M., Macdonald, K. D. and Bufton, A. W. J. (1953). The genetics of *Aspergillus nidulans*. *Adv. Genet.* **5**, 141-238.

Raymond, C. K., Howald-Stevenson, I., Vater, C. A. and Stevens, T. H. (1992). Morphological classification of the yeast vacuolar protein sorting mutants: evidence for a prevacuolar compartment in class E vps mutants. *Mol. Biol. Cell* **3**, 1389-1402.

Rieder, S. E., Banta, L. M., Kohrer, K., McCaffery, J. M. and Emr, S. D. (1996). Multilamellar endosome-like compartment accumulates in the yeast *vps28* vacuolar protein sorting mutant. *Mol. Biol. Cell* **7**, 985-999.

Rodríguez-Galán, O., Galindo, A., Hervás-Aguilar, A., Arst, H. N., Jr and Peñalva, M. A. (2009). Physiological involvement in pH signalling of Vps24-mediated recruitment of *Aspergillus* PalB cysteine protease to ESCRT-III. *J. Biol. Chem.* **284**, 4404-4412.

Rothfels, K., Tanny, J. C., Molnar, E., Friesen, H., Commisso, C. and Segall, J. (2005). Components of the ESCRT pathway, DFG16, and YGR122w are required for Rim101 to act as a corepressor with Nrg1 at the negative regulatory element of the *DIT1* gene of *Saccharomyces cerevisiae*. *Mol. Cell. Biol.* **25**, 6772-6788.

Rusten, T. E. and Stenmark, H. (2009). How do ESCRT proteins control autophagy? *J. Cell Sci.* **122**, 2179-2183.

Saksena, S., Wahlman, J., Teis, D., Johnson, A. E. and Emr, S. D. (2009). Functional reconstitution of ESCRT-III assembly and disassembly. *Cell* **136**, 97-109.

Shoji, J. Y., Maruyama, J., Arioka, M. and Kitamoto, K. (2005). Development of *Aspergillus oryzae thiA* promoter as a tool for molecular biological studies. *FEMS Microbiol. Lett.* **244**, 41-46.

Spathas, D. H. (1978). A salt sensitive mutation on chromosome VI of Aspergillus nidulans. *Aspergillus Newsletter* **46**, 28.

Spielvogel, A., Findon, H., Arst, H. N., Jr, Araujo-Bazán, L., Hernández-Ortiz, P., Stahl, U., Meyer, V. and Espeso, E. A. (2008). Two zinc finger transcription factors, CrzA and SltA, are involved in cation homoeostasis and detoxification in *Aspergillus nidulans*. *Biochem. J.* **414**, 419-429.

Szewczyk, E., Nayak, T., Oakley, C. E., Edgerton, H., Xiong, Y., Taheri-Talesh, N., Osmani, S. A. and Oakley, B. R. (2006). Fusion PCR and gene targeting in *Aspergillus nidulans*. *Nat. Protoc.* **1**, 3111-3120.

Teis, D., Saksena, S. and Emr, S. D. (2008). Ordered assembly of the ESCRT-III complex on endosomes is required to sequester cargo during MVB formation. *Dev. Cell* **15**, 578-589.

Teis, D., Saksena, S., Judson, B. L. and Emr, S. D. (2010). ESCRT-II coordinates the assembly of ESCRT-III filaments for cargo sorting and multivesicular body vesicle formation. *EMBO J.* **29**, 871-883.

Tilburn, J., Scazzocchio, C., Taylor, G. G., Zabicky-Zissman, J. H., Lockington, R. A. and Davies, R. W. (1983). Transformation by integration in *Aspergillus nidulans*. *Gene* **26**, 205-211.

Tilburn, J., Sarkar, S., Widdick, D. A., Espeso, E. A., Orejas, M., Mungroo, J., Peñalva, M. A. and Arst, H. N., Jr (1995). The *Aspergillus* PacC zinc finger transcription factor mediates regulation of both acid- and alkaline-expressed genes by ambient pH. *EMBO J.* **14**, 779-790.

Tilburn, J., Sánchez-Ferrero, J. C., Reoyo, E., Arst, H. N., Jr and Peñalva, M. A. (2005). Mutational analysis of the pH signal transduction component PalC of *Aspergillus nidulans* supports distant similarity to BRO1 domain family members. *Genetics* **171**, 393-401.

Uetz, P., Giot, L., Cagney, G., Mansfield, T. A., Judson, R. S., Knight, J. R., Lockshon, D., Narayan, V., Srinivasan, M., Pochart, P. et al. (2000). A comprehensive analysis of protein-protein interactions in *Saccharomyces cerevisiae*. *Nature* **403**, 623-627.

Vincent, O., Rainbow, L., Tilburn, J., Arst, H. N., Jr and Peñalva, M. A. (2003). YPXL/I is a protein interaction motif recognised by *Aspergillus* PalA and its human homologue AIP1/Alix. *Mol. Cell. Biol.* **23**, 1647-1655.

Weiss, P., Huppert, S. and Kolling, R. (2009). Analysis of the dual function of the ESCRT-III protein Snf7 in endocytic trafficking and in gene expression. *Biochem. J.* **424**, 89-97.

Wolf, J. M. and Davis, D. A. (2010). Mutational analysis of *Candida albicans SNF7* reveals genetically separable Rim101 and ESCRT functions and demonstrates divergence in bro1-domain protein interactions. *Genetics* **184**, 673-694.

Wollert, T. and Hurley, J. H. (2010). Molecular mechanism of multivesicular body biogenesis by ESCRT complexes. *Nature* **464**, 864-869.

Wollert, T., Wunder, C., Lippincott-Schwartz, J. and Hurley, J. H. (2009). Membrane scission by the ESCRT-III complex. *Nature* **458**, 172-177.

Xu, W. and Mitchell, A. P. (2001). Yeast PalA/AIP1/Alix homolog Rim20p associates with a PEST-like region and is required for its proteolytic cleavage. *J. Bacteriol.* **183**, 6917-6923.

Xu, W., Smith, F. J., Jr, Subaran, R. and Mitchell, A. P. (2004). Multivesicular body-ESCRT components function in pH response regulation in *Saccharomyces cerevisiae* and *Candida albicans*. *Mol. Biol. Cell* **15**, 5528-5537.

Yu, J. H., Hamari, Z., Han, K. H., Seo, J. A., Reyes-Domínguez, Y. and Scazzocchio, C. (2004). Double-joint PCR: a PCR-based molecular tool for gene manipulations in filamentous fungi. *Fungal Genet. Biol.* **41**, 973-981.

Journal of Cell Science